Available online at www.sciencedirect.com
SCIENCE DIRECT®
Journal of Solid State Chemistry 178 (2005) 1125–1132
JOURNAL OF SOLID STATE CHEMISTRY
www.elsevier.com/locate/jssc

Dimorphism in iron(II) methylphosphonate: Low-temperature crystal structure and temperature-dependent Mössbauer studies of a new form of the layered weak ferromagnet $Fe[(CH_3PO_3)(H_2O)]$

Philippe Léone[a,*], Pierre Palvadeau[a], Kamal Boubekeur[a], Alain Meerschaut[a], Carlo Bellitto[b], Elvira M. Bauer[b], Guido Righini[b], Pavel Fabritchnyi[c]

[a]*Laboratoire de Chimie des Solides, Institut des Matériaux Jean Rouxel, UMR CNRS 6502, 2, rue de la Houssiniere, B.P. 33229, FR-44322 Nantes, Cedex 3, France*
[b]*CNR—Istituto di Struttura della Materia, via Salaria Km 29.5, C.P. 10, I-00016, Monterotondo Stazione (Roma), Italy*
[c]*Department of Chemistry, M.V. Lomonosov Moscow State University, 119899 Moscow V-234, Russia*

Received 8 November 2004; received in revised form 19 January 2005; accepted 21 January 2005

Abstract

A second form of the literature-known layered weak ferromagnet $Fe[(CH_3PO_3)(H_2O)]$ has been isolated. The crystal structure determination of this new form (**2**) has been carried out at $T = 300$, 200 and 130 K. It crystallizes in the orthorhombic space group $Pmn2_1$: $a = 5.7177(11)$, $b = 8.8093(18)$, $c = 4.8154(10)$ Å, while form (**1**) crystallizes in the space group $Pna2_1$: $a = 17.58(2)$, $b = 4.814(1)$, $c = 5.719(1)$ Å. Mössbauer spectroscopy on form (**2**) has been performed in the temperature range 4–300 K; and, at $T \sim 160$ K, a drastic change in the quadrupole splitting (ΔE) and a broadening of the doublet components is noticed. But surprisingly, on cooling the crystal, no structural change is observed, which could account for the increase in ΔE. Below $T = 25$ K, ^{57}Fe spectra transform into hyperfine splitting patterns which reveal a magnetically ordered state in agreement with the results of earlier magnetic susceptibility studies.

Keywords: Iron phosphonate; Polymorphs; Crystal structure; Mössbauer spectroscopy

1. Introduction

Metal phosphonates $M[(RPO_3)(H_2O)]$ and bis(phosphonates) $M_2[(O_3PRPO_3)(H_2O)_2]$ (M = divalent metal ion, R = alkyl or aryl group) are typical examples of hybrid organic–inorganic compounds and have been intensively studied in the recent past for several reasons. They can be used as ion exchangers, catalysts, or as hosts in intercalation compounds, and they have also provided interesting examples of low-dimensional magnetic compounds [1–3]. Single crystal structures of a few iron(II) and iron(III) phosphonates have been previously solved either from crystal or powder X-ray diffraction (PXRD) data studies [3–6]. The structural network of this class of compounds is lamellar and it consists of inorganic layers, separated by organic moieties along one direction of the unit cell. On increasing the number of carbon atoms in the R group of the phosphonate ligand, the thickness of the organic layers increases and, as a consequence, the distance increases as well. The inorganic layers are made of metal cations in octahedral coordination by six oxygen atoms, five from phosphonate groups and one from a water molecule. Since the compound contains only one phosphonate per metal ion, all the phosphonate oxygen atoms take part in the metal binding and two oxygen atoms chelate the metal ion and at the same time bridge

*Corresponding author. Fax: +33 240373995.
E-mail address: philippe.leone@cnrs-imn.fr (P. Léone).

0022-4596/$ - see front matter © 2005 Elsevier Inc. All rights reserved.
doi:10.1016/j.jssc.2005.01.020

adjacent metal ions in the same row. Oxygen of the phosphonate lying in the mirror plane bonds only to one Fe atom and it is located trans to the oxygen of the water molecule which is also coordinated to the metal ions. This arrangement originates the crenelated inorganic layer. From a magnetic point of view, iron(II) phosphonate compounds are known as "canted antiferromagnets" or "weak ferromagnets" [7]. The ordering temperature has been found to be around $T_N \sim 25$ K and is independent on the interlayer distance in the lattice [6].

The undoubted advantage of iron phosphonates is due to the fact that they contain ^{57}Fe Mössbauer probe which provides valuable information about the oxidation state, the symmetry of the site, the magnetic ordering temperature and hyperfine field at iron atoms. Quite recently iron(II) methylphosphonate, i.e., $Fe[(CH_3PO_3)(H_2O)]$, has been prepared and the crystal structure solved at room temperature (form (**1**)) [6]. The transparent platelets were found to crystallize in the orthorhombic space group $Pna2_1$. Quite interesting, this form (**1**) crystallizes together with a second modification, form (**2**), which represents the object of the present study. As far as we know, this is the first time that two different crystalline forms of the same iron(II) alkylphosphonate were isolated and structurally characterized from the same preparation.

In this paper, the results of both the X-ray single crystal determination at room temperature and at low temperatures and Mössbauer spectroscopy characterization of the second crystal modification of the iron(II) methylphosphonate, $Fe[(CH_3PO_3)(H_2O)]$, form (**2**), are reported.

2. Experimental

Methylphosphonic acid, $CH_3PO_3H_2$, was of analytical grade (*Aldrich Chemical Co.*) and used without further purification. HPLC water was used as solvent. All reactions involving Fe(II) ion were carried out under inert atmosphere using conventional Schlenck techniques. Elemental analyses were performed by Malissa and Reuter Mikroanalytische Laboratorien, Elbach, Germany. The IR and UV–visible spectra were recorded with a Perkin–Elmer FTIR 16F and a Varian Cary 5 spectrophotometer, respectively.

2.1. Crystal growth of $Fe[(CH_3PO_3)(H_2O)]$

The preparation of the compound has been described previously [6]. The growth of a suitable single crystal was carried out by heating up to 90 °C from 12 to 14 days a sealed ampoule containing a degassed water solution (30 mL) of $[FeSO_4] \cdot 7H_2O$ (1.33 g, 4.8 mmol), $CH_3PO_3H_2$ (0.51 g, 5.3 mmol) and urea (0.51 g, 8.5 mmol). Colorless platelets and needle-like crystals were isolated, filtered and dried in air. The pH of the final filtrate solution was found to be 7.55.

As mentioned above two different types of crystals were identified: the first form, hereafter form (**1**), made of white platelets, crystallizes in the orthorhombic space group $Pna2_1$ with the following unit-cell parameters: $a = 17.58(2)$ Å, $b = 4.814(1)$ Å, $c = 5.719(1)$ Å. The second form, i.e., form (**2**) crystallizes as needle-like crystals in the orthorhombic space group $Pmn2_1$ with the following unit-cell parameters: $a = 5.7177(11)$ Å, $b = 8.8093(18)$ Å, $c = 4.8154(10)$ Å.

The identification and the presence of both forms in the same sample were also confirmed by X-ray powder diffraction studies (see below).

The preparation of the compound gives mainly form (**2**) if reaction is carried out in a more concentrated starting solution. The pH of the final solution was found to be 7.4. Needle-like colorless crystals stable in air at room temperature were isolated. A JEOL 5800 scanning electron microscope equipped with a PGT microanalyzer was used to check the P/Fe ratio in several crystals, including the crystal used for the structure determination. In any case the ratio was found to be very close to **1**.

2.2. X- ray structure determination and powder characterization

The crystal structure of the second form of $Fe[(CH_3PO_3)(H_2O)]$ has been studied and solved at three different temperatures. The crystal used for the X-ray diffraction studies was a colorless needle of dimensions $(0.1 \times 0.1 \times 0.3)$ mm^3. Due to the size of the crystal and the weak value of the linear absorption coefficient ($\mu = 3.3$ cm^{-1}), no correction for absorption was carried out. The reflection intensities were collected at different temperatures (i.e., 300, 200, 130 K) on a Nonius Kappa CCD X-ray diffractometer system equipped with a graphite monochromatized Mo$K\alpha_1$ radiation ($\lambda = 0.71073$ Å). Crystal data at low temperatures were collected with an Oxford 700 series cryostat cooler associated to an Oxford AD41 dry air unit. The structures were solved by means of the direct methods and all subsequent calculations were carried out with the SHELXL 97 program [8].

Experimental PXRD data were collected with two different instrumentations in two laboratories (Nantes, Rome):

- Room temperature PXRD data collected in Nantes were recorded on an INEL CPS120-equipped diffractometer in a horizontal Debye–Scherrer geometry, with a quartz monochromator, Cu$K\alpha_1$ radiation. CPS120 is a curve gaseous detector designed around a blade anode [9]. Experimental data have been

obtained on a Lindemann capillary filled with the sample. Simulated spectra were calculated from atomic positions, cell parameters and space groups given for both structural determinations, using the FULLPROF program [10] (Fig. 2a).

- Room temperature PXRD data collected in Rome were recorded on a Seifert XRD-3000 diffractometer, Bragg–Brentano geometry, equipped with a curved graphite monochromator [$\lambda(\mathrm{Cu}K\alpha_1) = 1.5406$ Å] and a scintillation detector. The data were collected with a step size of 0.02°, 2θ and at count time of 8 s per step over the range $4° < 2\theta < 80°$. The sample was mounted on a flat glass plate, giving rise to a strong preferred orientation. The diffractometer zero point was determined from an external Si standard. PXRD patterns were fitted by using the POWDERCELL program [11] (Fig. 2b).

2.3. Mössbauer spectroscopy

Mössbauer spectra were obtained with a constant acceleration automatic folding Elscint-type spectrometer using a room-temperature ^{57}Co(Rh) source in transmission geometry and a triangular reference signal. α-Fe was used as reference. Samples were studied in the 4–300 K temperature range with an Oxford Instrument variable temperature cryostat. The spectra were computed with a least squares routine using Lorentzian lines. Three different velocity scales were used to obtain an acceptable precision in the paramagnetic state (4.08 mm/s at 300 K, 5.84 mm/s between 32 and 280 K) and in the ordered domain (7.54 mm/s).

3. Results and discussion

3.1. Single-crystal structure determination of form (2) as a function of temperature

In order to understand the Mössbauer results, which showed an anomalous increase in the quadrupole splitting around 150 K, an X-ray crystal study has been undertaken at 200 and 130 K in addition to that at room temperature (i.e., 300 K). In lamellar compounds, interlayer spaces are generally temperature dependent, and when water molecules are present in the structure, orientations and disorders are expected to be frozen at low temperatures.

The previously reported crystal structure of form (**1**) Fe[$(CH_3PO_3)(H_2O)$] [6] was solved in the orthorhombic symmetry, space group $Pna2_1$. In this work, needle-like crystals of form (**2**) have been selected from the sample used for Mössbauer spectroscopy and studied with a Kappa CCD diffractometer. Several crystals have been tested, and all of them were found to crystallize in space group $Pmn2_1$. A suitable crystal was then selected for structure determination. At 300 K, in the orthorhombic symmetry, the unit-cell parameters are: $a = 5.7177(11)$ Å, $b = 8.8093(18)$ Å, $c = 4.8154(10)$ Å. Details of data collection are given in Table 1. It is noteworthy that $(NH_4)FePO_4$ and Fe[$(C_6H_5PO_3)(H_2O)$] both crystallize in the same space group $Pmn2_1$ [5,12]. The crystal structure of form (**2**) consists of alternating organic and inorganic layers along the b direction of the unit cell. Fig. 1 shows projections of the two structures, i.e., form (**1**) and form (**2**), at 300 K. The difference between the two forms lies in the ligand arrangement. In form (**2**), the C–P bond above the inorganic layer is approximately 12° away from the normal axes of the inorganic layers, keeping the same orientation from layer to layer along the b-direction. The a parameter of form (**1**) is twice larger than the corresponding b parameter of form (**2**) because there is an alternation of the inclination of the C–P bond in a zigzag way (see Fig. 1). The hydrogen positions of the methyl group were found from the AFIX instruction (the default C–H distance is 0.96 Å). The hydrogen positions of the water molecule have been found through the DFIX instruction. All non-hydrogen atom positions have been anisotropically refined; positions for all the hydrogen atoms have been refined. Final refinement resulted in value of $R_1 = 0.044$ for 1015 reflections ($I > 2\sigma(I)$) and 48 parameters. Results are reported in Table 2, together with those obtained at 200 and 130 K. The

Table 1
Crystal data and structure refinement for Fe[$(CH_3PO_3)(H_2O)$] form (**2**) at 300 K

Identification code	Fe methylphosphonate form (**2**)
Empirical formula	Fe[$(CH_3PO_3)(H_2O)$]
Formula weight (g/mol)	167.87
Temperature (K)	293
Wavelength (Å)	0.71073
Crystal system	Orthorhombic
Space group	$Pmn2_1$
Unit cell dimensions (Å)	$a = 5.718(1)$; $b = 8.809(2)$; $c = 4.815(1)$
Volume (Å^3)	242.55(8)
Z	2
Density (calculated)	2.299
Absorption coefficient (mm^{-1})	3.335
$F(000)$	168
Crystal size (mm^3)	$0.1 \times 0.1 \times 0.3$
Theta range for data collection	4.25–34.96°
Index ranges	$-8 \leqslant h \leqslant 9$, $-14 \leqslant k \leqslant 9$, $-7 \leqslant l \leqslant 7$
Reflections collected	4736
Independent reflections	1099 [R(int) = 0.0789]
Completeness to theta = 34.96°	99.7%

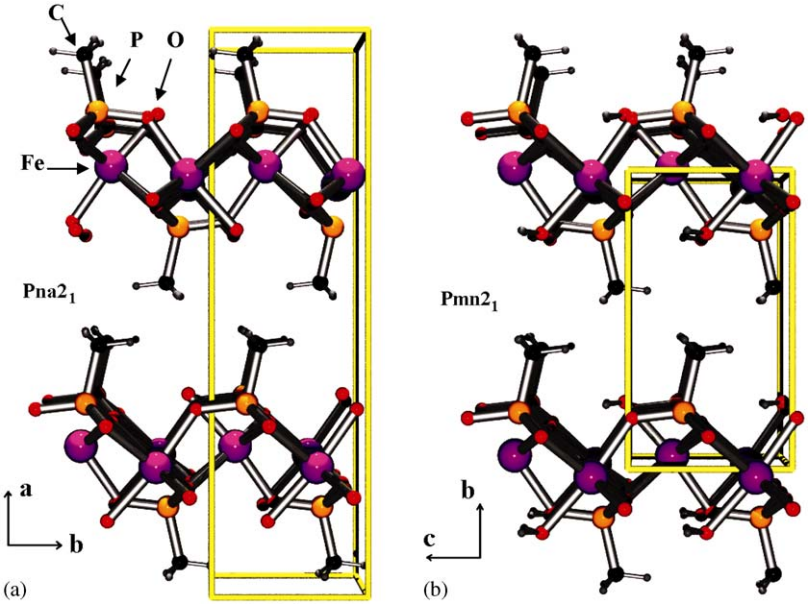

Fig. 1. The crystal structures of form (**1**) (a), and form (**2**) (b) of Fe[$(CH_3PO_3)(H_2O)$].

Table 2
Structure solution and refinement for Fe[$(CH_3PO_3)(H_2O)$] form (**2**) at 300, 200 and 130 K

	300 K	200 K	130 K
Refinement method	Full-matrix least-squares on F^2		
Data/restraint/parameter	1099/10/48	873/10/48	859/10/48
Goodness-of-fit on F^2	1.098	1.108	1.135
Final R indices for 1015 reflections [$I>2\sigma(I)$]	$R_1 = 0.044$, w$R_2 = 0.106$	$R_1 = 0.074$, w$R_2 = 0.204$	$R_1 = 0.039$, w$R_2 = 0.098$
R indices for 1099 reflections (all data)	$R_1 = 0.050$, w$R_2 = 0.111$	$R_1 = 0.082$, w$R_2 = 0.215$	$R_1 = 0.040$, w$R_2 = 0.099$
Flack x parameter	−0.02 (3)	0.01 (7)	−0.03 (4)
F.D.: highest peak and deepest hole (e/Å^3)	1.38 and −1.37	2.06 and −4.04	1.19 and −1.29

poor quality of the results at 200 K could be related with a bad crystal centering when cooling, leading to bad integrated intensities and consequently to a relatively high R factor and high residuals. Table 3 gathers atomic positions and equivalent isotropic displacement parameters for the three temperatures. The main distances and angles around iron atoms are reported in Table 4. The crystalline network and space group in form (**2**) does not change on cooling and only a small variation of crystal parameters is observed. The structures determined at these three different temperatures are quasi-identical. Despite the doubling of one parameter for form (**1**) and a different space group, both forms show a quite similar structure.

3.2. Powder X-ray diffraction studies

PXRD data were collected on pure Fe[$(CH_3PO_3)(H_2O)$] form (**2**) sample, used also for Mössbauer experiments (see Fig. 2a), as well as on powder sample obtained from a more concentrated solution (see Fig. 2b). Fig. 2a shows the experimental PXRD data together with the simulated PXRD diagrams of pure form (**1**) (i.e., space group $Pna2_1$), and pure form (**2**) (i.e., space group $Pmn2_1$). Some specific diffraction lines are present in the simulated powder diagram of form (**1**) but not in form (**2**); the most evident lines are: (111) at $2\theta = 24.70^\circ$, (311) at $2\theta = 28.61^\circ$ and (511) at $2\theta = 35.25^\circ$. These diffraction lines are absent from the experimental powder diagram. This result identifies the crystalline sample as a pure form (**2**) on which the Mössbauer spectra were recorded. In the sample obtained from less concentrated solution (see Fig. 2b), the characteristic $Pna2_1$ diffraction lines are visible in the experimental pattern, indicating the presence of a mixture of both forms.

3.3. Mössbauer spectroscopy

^{57}Fe Mössbauer spectra of Fe[$(CH_3PO_3)(H_2O)$] form (**2**) were investigated over the temperature range 4.2–300 K. The obtained results allow to select two different domains corresponding to the paramagnetic

Table 3
Atomic coordinates and equivalent isotropic displacement parameters (10^{-3} Å^2) for Fe[$(CH_3PO_3)(H_2O)$] form (**2**) at 300, 200 and 130 K

	x	y	z	U(eq)
300 K				
Fe(1)	0	0.9749(1)	0.2229(2)	17(1)
P(1)	0	0.1911(1)	0.6611(2)	15(1)
O(1)	0	0.1709(4)	−0.0265(7)	21(1)
O(2)	0.2145(5)	0.1171(3)	0.5177(5)	21(1)
C(1)	0	0.3883(6)	0.5805(14)	35(1)
H(1A)	0	0.397(11)	0.382(4)	53
H(1B)	0.137(3)	0.433(6)	0.662(9)	53
O(3)	0	0.7882(5)	0.5223(10)	25(1)
H(3)	0.127(3)	0.794(6)	0.640(6)	38
200 K				
Fe(1)	0	0.9748(1)	0.2231(3)	13(1)
P(1)	0	0.1921(2)	0.6600(5)	11(1)
O(1)	0	0.1718(9)	−0.0261(18)	17(1)
O(2)	0.2143(9)	0.1177(5)	0.5195(13)	17(1)
C(1)	0	0.3910(11)	0.579(3)	28(2)
H(1A)	0	0.38(2)	0.378(6)	42
H(1B)	0.136(3)	0.443(8)	0.639(18)	42
O(3)	0	0.7884(9)	0.524(2)	19(1)
H(3)	0.129(3)	0.778(11)	0.635(9)	28
130 K				
Fe(1)	0	0.9746(1)	0.2231(2)	8(1)
P(1)	0	0.1930(1)	0.6603(2)	8(1)
O(1)	0	0.1732(5)	−0.0248(9)	12(1)
O(2)	0.2148(5)	0.1182(3)	0.5181(6)	13(1)
C(1)	0	0.3911(6)	0.5781(13)	16(1)
H(1A)	0	0.404(9)	0.380(4)	24
H(1B)	0.138(3)	0.435(5)	0.660(9)	24
O(3)	0	0.7874(5)	0.5246(9)	13(1)
H(3)	0.128(3)	0.793(5)	0.642(7)	19

U(eq) is defined as one-third of the trace of the orthogonalized U_{ij} tensor.

Table 4
Selected interatomic distances (Å) for Fe[$(CH_3PO_3)(H_2O)$] form (**2**) at 300, 200 and 130 K

	300 K	200 K	130 K
Fe–O(1)	2.103(4)	2.102(8)	2.105(4)
Fe–O(2)	2 × 2.256(3)	2 × 2.267(6)	2 × 2.254(3)
	2 × 2.073(3)	2 × 2.086(5)	2 × 2.067(3)
Fe–O(3)	2.188(4)	2.184(9)	2.185(4)
C–H(1A)	0.96(2)	0.96(2)	0.96(2)
C–H(1B)	2 × 0.96(1)	2 × 0.96(1)	2 × 0.96(1)
O(3)–H(3)	2 × 0.92(1)	0.92(1)	2 × 0.92(1)

state and the magnetically ordered state of iron moments.

3.3.1. Paramagnetic domain

X-ray single crystal structure determination at room temperature of the title compound showed that iron is located on a single crystallographic position in a distorted oxygen octahedron. Mössbauer spectroscopy data of form (**2**) are consistent with this finding.

At $T = 300$ K, the spectrum (Fig. 3) consists of a single doublet whose parameters (the isomer shift $\delta = 1.20 \pm 0.01$ mm/s, the quadrupole splitting $\Delta E = 1.49 \pm 0.02$ mm/s, the half-width at half-maximum of each doublet component ($\gamma = 0.12 \pm 0.02$ mm/s) are typical of a high-spin Fe^{2+} ion in a distorted octahedral surrounding. This spectrum thus ascertains the occurrence of iron in a unique oxidation state on a site of unique type. The doublet components are of unequal intensities but the asymmetry could be suppressed by a rotation of the sample to the magic angle towards the observation axis. This means that the asymmetry of the doublet is essentially due to orientation effects related to lamellar morphology of crystallites.

At $T = 200$ K, the parameters of the spectrum ($\delta = 1.27 \pm 0.01$ mm/s, $\Delta E = 1.69 \pm 0.01$ mm/s, $\gamma = 0.18 \pm 0.02$ mm/s) do not show any anomalous change. In fact, the observed small increase in δ value is assignable to the second-order Doppler shift occurring upon lowering the measurement temperature. As for the increase in the ΔE value, it is consistent with usual temperature dependence of the valence contribution in the electric field gradient EFG for Fe^{2+}.

At $T = 120$ K, the spectrum ($\delta = 1.31 \pm 0.01$ mm/s, $\Delta E = 2.73 \pm 0.01$ mm/s, $\gamma = 0.19 \pm 0.02$ mm/s) shows that the ΔE value is obviously different from that at 300 K (Fig. 4). This emphasizes the fact that quadrupole interaction of ^{57}Fe depends on the distribution of the sixth electron of Fe(II) over half-filled t_{2g} orbitals. One can notice that crystal field effects of comparable magnitude were reported by Ingalls [13 and ref. therein] for ^{57}Fe in $Fe(NH_4)_2(SO_4)_2 \cdot 6H_2O$.

Surprisingly, the measurements performed between 120 and 200 K have revealed, in the vicinity of 160 K, the occurrence of a drastic change in ΔE (Fig. 4) and an anomalous broadening of the doublet components (Fig. 3) ($\delta = 1.29 \pm 0.01$ mm/s, $\Delta E = 1.86 \pm 0.02$ mm/s, $\gamma = 0.42 \pm 0.02$ mm/s). These changes imply the existence of a process strongly affecting the value of EFG. It is noteworthy that a similar evolution has been previously observed in the Fe(II) ethylphosphonate, Fe[$(C_2H_5PO_3)(H_2O)$] [14], but the transition occurred in a wider temperature range, from 125 to 200 K. The origin of the "anomalous" behavior of ΔE remains an open question. One can suppose, however, that it is to be related to thermally activated water molecule motion. The large ΔE and narrow absorption lines at $T \ll 160$ K would correspond to the quadrupole interaction in a "frozen" H_2O conformation. The narrow absorption lines and smaller ΔE at $T \gg 160$ K would correspond to a conformation relaxation which is fast compared to the ^{57m}Fe nuclear lifetime. The broadened absorption lines in the vicinity of 160 K would reflect intermediate relaxation rates. Such a hypothesis had in fact permitted

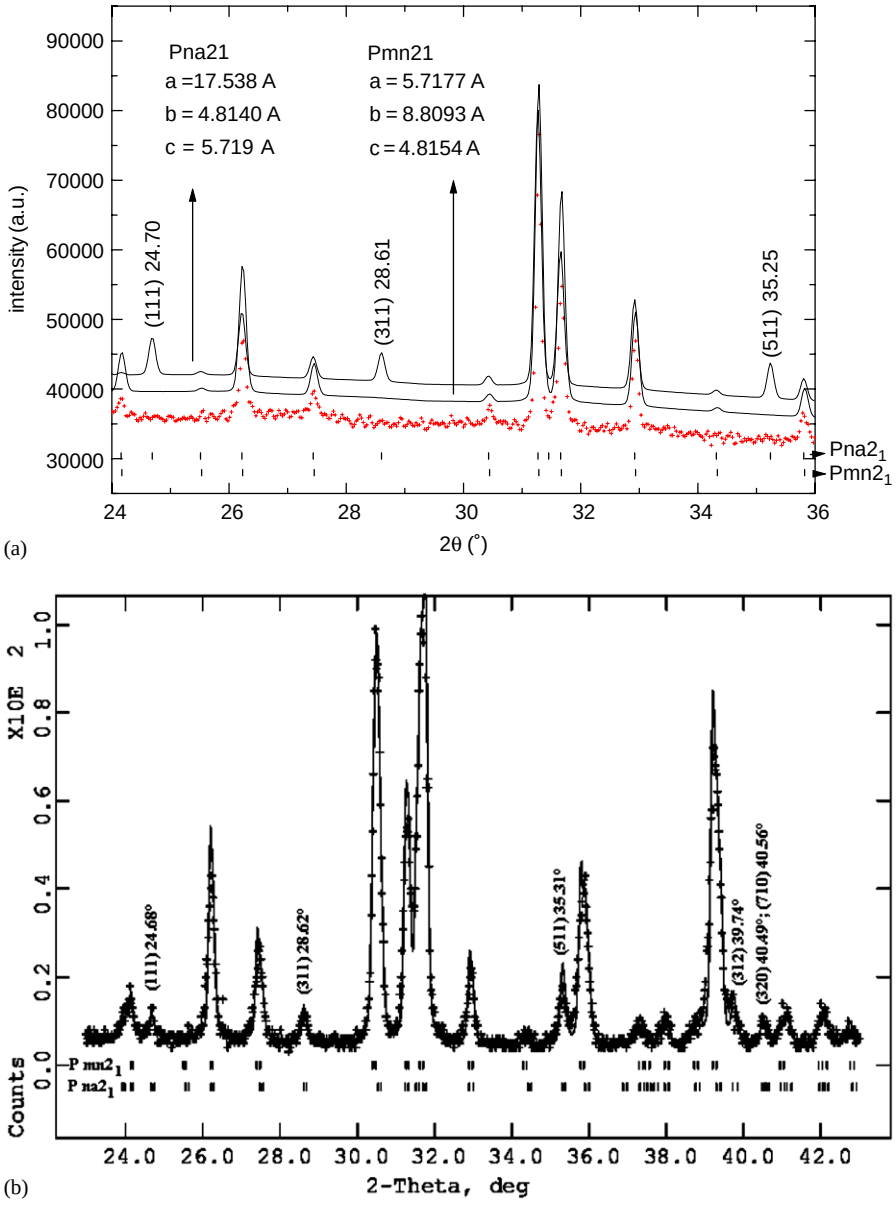

Fig. 2. (a) Experimental X-ray powder diffraction pattern (+ + + +) of a sample used for Mössbauer studies, with the XRDP simulations (continuous line) assuming *Pna*2$_1$ and *Pmn*2$_1$ space groups. (b) Experimental X-ray powder diffraction pattern of a sample containing both the needle-like (form (**2**) and platelets form (**1**) (+ + + +) and fitting curve (continuous line).

to account for the temperature dependence of ΔE in [Fe(O_2)(N–Me-imide)(α,α,α,α-TpivPP)] [15].

3.3.2. Ordered domain

Finally, at $T \leqslant 25$ K ^{57}Fe spectra transform into hyperfine splitting patterns which reveal the presence of a magnetically ordered state. Magnetic susceptibility measurements performed also on a single crystal of form (**1**) and on a microcrystalline powder sample containing mainly form (**1**) confirmed the magnetic transition temperature (unpublished results). At 4.2 K, the spectrum (Fig. 3) is of rather particular shape which reflects the combined magnetic and quadrupole interaction. Being fitted within approximation of full Hamiltonian, it leads to a low hyperfine field $H = 160 \pm 5$ kOe, a large quadrupole coupling constant $eV_{zz}Q \cong 2|\Delta E| = +6.1 \pm 0.1$ mm/s and an angle θ between H and V_{zz} of $65 \pm 5^\circ$. These parameters would provide further information about local surrounding of iron if the magnetic structure of form (**2**) was solved.

4. Conclusions

In this contribution, we have demonstrated the existence of dimorphism in iron(II) methylphosphonate derivative. As far as we know, this is the first time in the

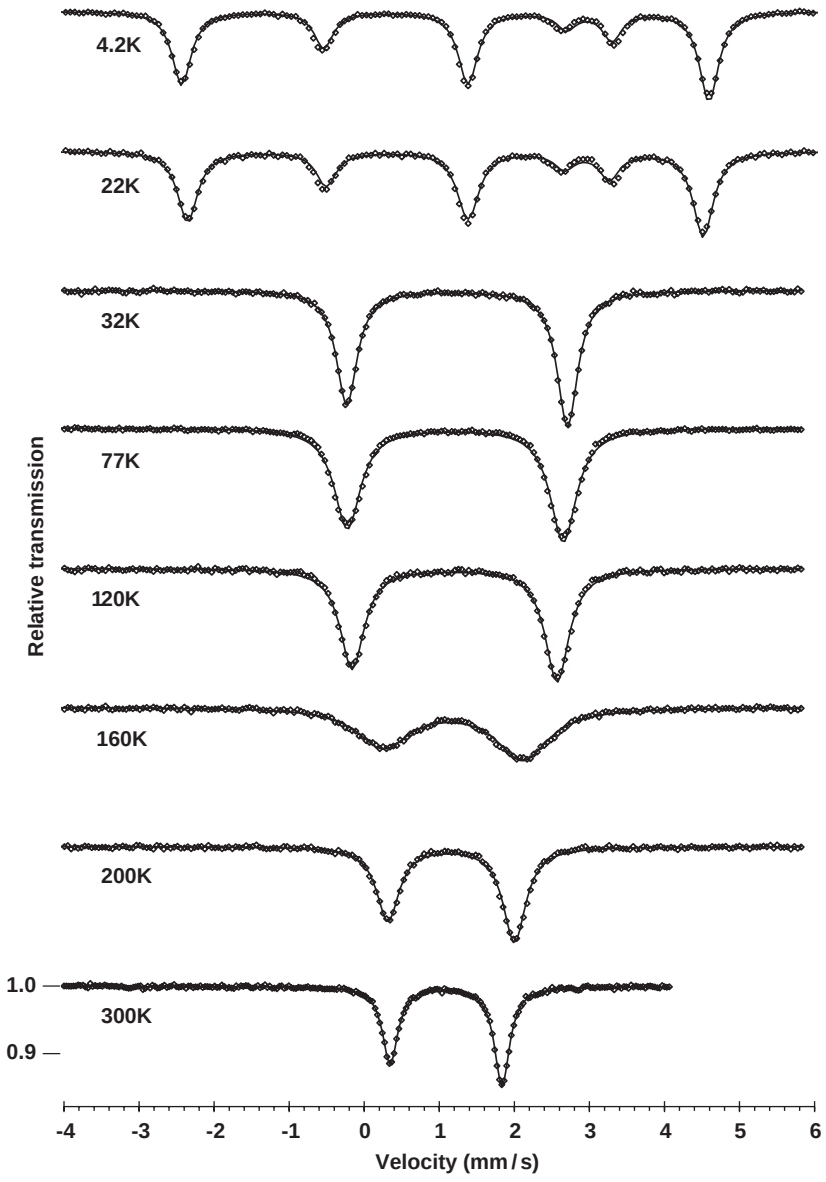

Fig. 3. Mössbauer spectra of Fe[$(CH_3PO_3)(H_2O)$] form (**2**) at different temperatures. Three different velocity scales were used: 4.08 mm/s at 300 K, 5.84 mm/s between 32 and 200 K and 7.54 mm/s at 4.2 K.

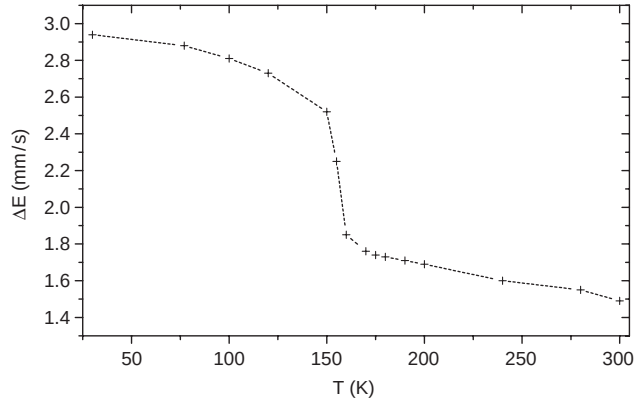

Fig. 4. Evolution of the quadrupole splitting ΔE (mm/s) versus temperature.

class of metal(II) phosphonates that two polymorphic forms were isolated and structurally characterized. Form (**2**) is easier to prepare and crystallizes as colorless needles, while form (**1**) grows as platelets. The new form (**2**) of Fe[$(CH_3PO_3)(H_2O)$] has been isolated and characterized. Its space group $Pnm2_1$ has been previously observed in several other layered divalent metal alkylphosphonates, such as Cd[$(CH_3PO_3)(H_2O)$], Fe[$(C_6H_5PO_3)(H_2O)$], and Ni[$(CH_3PO_3)(H_2O)$] [3,5,16]. The crystal structure of form (**2**) has been studied and solved at three different temperatures, in an attempt to correlate the structural results with Mössbauer data obtained in the relevant temperature range. The temperature evolution of ^{57}Fe quadrupole splitting points to the occurrence of a process which drastically

influences the value of the electric field gradient at Fe(II) nuclei in the vicinity of 160 K.

Acknowledgments

This work has been supported by the French CNRS (Institut des Matériaux de Nantes) and by the Italian CNR (Istituto di Struttura della Materia). The Italian Ministry of the University and Research FIRB 2001 programme on "Ibridi organici inorganici funzionali" and European COST D14 program are acknowledged for the financial support.

References

[1] G. Alberti, in: J.M. Lehn (Ed.), Comprehensive Supramolecular Chemistry, vol. 7, Pergamon Press, New York, 1996, pp. 151–187.
[2] A. Clearfield, Prog. Inorg. Chem. 47 (1998) 371–510.
[3] (a) G. Cao, H. Lee, V.M. Lynch, T.E. Mallouk, Inorg. Chem. 27 (1981) 2781–2785;
(b) G. Cao, H. Lee, V.M. Lynch, L.M. Yacullo, Chem. Mater. 5 (1993) 1000–1006;
(c) K.J. Martin, P.J. Squattrito, A. Clearfield, Inorg. Chim. Acta 155 (1989) 7–9.
[4] (a) B. Bujoli, O. Pena, P. Palvadeau, J. Le Bideau, C. Payen, J. Rouxel, Chem. Mater. 5 (1993) 583–587;
(b) J. Le Bideau, C. Payen, B. Bujoli, P. Palvadeau, J. Rouxel, J. Magn. Magn. Mater. 140 (1995) 1719–1720.
[5] A. Altomare, C. Bellitto, S.A. Ibrahim, R. Rizzi, Inorg. Chem. 39 (2000) 1803–1808.
[6] C. Bellitto, F. Federici, M. Colapietro, G. Portatone, D. Caschera, Inorg. Chem. 41 (2002) 709–714.
[7] (a) R.L. Carlin, in: Magnetochemistry, Springer, Berlin, 1986;
(b) C.G. Shull, W.A. Stranser, E.O. Wollan, Phys. Rev. 83 (1951) 333–345;
(c) T. Moriya, Phys. Rev. 120 (1960) 91–98.
[8] G.M. Sheldrick, SHELXTL V, Siemens Analytical X-Ray Instruments, Madison, WI, 1997.
[9] J. Ballon, V. Comparat, J. Pouxe, Nucl. Instrum. Methods 217 (1983) 213–216.
[10] J. Rodriguez-Carvajal, Abstracts of the Satellite Meeting on Powder Diffraction of the XV Congress of the IUCr, Toulouse, 1990, p. 127.
[11] W. Kraus, G. Nolze, PowderCell for Windows, vers. 2.4, http://www.ccp14.ac.uk/ccp/web-mirrors/powdcell(a_v/v_1/powder/e_cell.html.
[12] J.E. Greedan, K. Reubenbauer, T. Birchall, M. Ehlert, J. Solid State Chem. 77 (1988) 376–388.
[13] R. Ingalls, Phys. Rev. 133 (1964) 787–795.
[14] P. Palvadeau, M. Queignec, B. Bujoli, V. Papaefthymiou, T. Bakas, Mater. Res. Bull. 31 (1996) 521–526.
[15] G. Long, K. Spartalian, in: E.G. Gruverman, C.W. Seidel (Eds.), Mössbauer Effect Methodology, vol. 10, Plenum press, New York, 1976, pp. 169–181.
[16] C. Bellitto, E.M. Bauer, S.A. Ibrahim, M.R. Mahmoud, G. Righini, Chem. Eur. J. 9 (2000) 1324–1331.